Liquid Crystals
Publication details, including instructions for authors and subscription information:
http://www.informaworld.com/smpp/title~content=t713926090

Layer and director structure in surface stabilized ferroelectric liquid crystal cells with non-planar boundary conditions

T. P. Rieker[a]; N. A. Clark[a]; G. S. Smith[ab]; C. R. Safinya[b]
[a] Condensed Matter Laboratory, Dept. of Physics and Center for Optoelectronic Computing Systems, University of Colorado, Boulder, Colorado, U.S.A. [b] Exxon Research and Engineering Co., Annandale, New Jersey, U.S.A.

To cite this Article Rieker, T. P. , Clark, N. A. , Smith, G. S. and Safinya, C. R.(1989) 'Layer and director structure in surface stabilized ferroelectric liquid crystal cells with non-planar boundary conditions', Liquid Crystals, 6: 5, 565 — 576
To link to this Article: DOI: 10.1080/02678298908034176
URL: http://dx.doi.org/10.1080/02678298908034176

LIQUID CRYSTALS, 1989, VOL. 6, NO. 5, 565–576

Layer and director structure in surface stabilized ferroelectric liquid crystal cells with non-planar boundary conditions

by T. P. RIEKER,† N. A. CLARK,† G. S. SMITH†‡ and C. R. SAFINYA‡

†Condensed Matter Laboratory, Dept. of Physics and Center for Optoelectronic Computing Systems, University of Colorado, Boulder, Colorado 80309-0390, U.S.A.

‡Exxon Research and Engineering Co., Route 22 East, Annandale, New Jersey 08801, U.S.A.

(*Received 31 January 1989; accepted 2 June 1989*)

High resolution X-ray scattering studies of thin smectic C* (SC) samples prepared between solid plates coated with obliquely evaporated silicon monoxide to favor surface director orientation tilted out of the surface plane, reveal a local layer structure which is dependent on the evaporation directions on the plates. Samples with the evaporation directions antiparallel exhibit uniformly tilted layers. Those with parallel evaporation directions exhibit a zig-zag defect free chevron structure of tilted layers.

1. Introduction

In this paper we present new information concerning the influence of surface interactions on the layer organization obtained in Surface Stabilized Ferroelectric Liquid Crystal (SSFLC) electro-optic cells. In an SSFLC cell a thin film of chiral (ferroelectric) SC liquid crystal (FLC) is the dielectric in a transparent capacitor formed by a pair of solid bounding plates. Such cells, when sufficiently thin, exhibit high speed, bistable electro-optic switching [1].

In SSFLC cells surface interactions have a dual function. The stable orientation states of the director **n**–polarization **P** field are stabilized by surface interactions at the FLC-plate interface [1, 2, 3]. Additionally the surfaces are used to produce layer alignment (layer intersections with the plates normal to a selected direction). The dual role of the FLC-surface interactions has made it particularly difficult to develop satisfactory SSFLC surface alignment treatments, typical problems being the appearance of novel textural defects such as zig-zag walls [3] or the dependence of switching characteristics on surface treatment. Such problems can be systematically solved only if the local layer structure (LLS) obtained with a given surface treatment is known. These considerations have led us to apply X-ray scattering to directly probe the LLS in SSFLC cells [4, 5, 6].

Our initial X-ray experiments have shown a remarkable 'chevron' LLS to be present in cells with surface treatments which orient **n** to be parallel to the glass surface (*planar* alignment, $\Omega = 0$ where Ω is the angle between **n** and the surface plane.) In addition, these studies have enabled us to understand in detail the full three dimensional nature of the 'zig-zag' layering defects which are prevalent in planar aligned cells [5], mediating changes in chevron direction. In this letter we extend our work to cells in which the surfaces have been treated via oblique silicon monoxide (SiO) deposition.

0267-8292/89 $3.00

Oblique evaporation of SiO is a well known technique for producing surfaces that strongly orient the nematic LC phase and has been applied to the smectic phases [7, 8]. The preferred orientation of **n** at the LC–SiO surface depends on the angle of incidence, θ_d, of deposition of the SiO layer. For θ_d larger than $\approx 80°$ (near grazing incidence) **n** is aligned in the plane of incidence at an angle $\Omega \approx 20°$, pointing toward the SiO evaporation source [9]. FLC phases aligned with such obliquely deposited SiO are of special interest because with antiparallel SiO evaporation directions on the two plates the layers are uniformly tilted rather than chevron [8, 10, 11, 12], and therefore zig-zag free [8]. In this paper we detail our briefly discussed earlier observations of the LLS in SiO cells [10] and extend them to report on the LLS present in a variety of SiO SSFLC cells, comparing the SiO results with those obtained from planar alignment on the same FLC materials.

2. X-ray scattering experiments

2.1. *Experimental details*

The experimental high resolution X-ray scattering geometry and planar sample cell preparation were as previously described [4, 6]. For those cells with an SiO alignment layer, both plates were coated with ≈ 300 Å of SiO (as determined by a quartz thickness monitor intercepting the SiO beam at normal incidence) deposited at an 82° angle of incidence. In assembly of the cells the direction of evaporation on the two plates was aligned either parallel (P–SiO) or antiparallel (A–SiO). The SiO coated plates were spaced by Mylar strips to avoid contamination with polymers or solvents. Cells were filled in the isotropic phase with one of the following commercial mixtures, Chisso CS-1014 [13], Merck ZLI-3654 [14], and BDH SCE-3 [15], then cooled into the underlying liquid crystal phases. The director orientation in the nematic phase is preserved as the sample is cooled into the SA phase. Cells were evaluated optically to ensure uniform alignment and that the bulk ferroelectric helix was suppressed. Experiments were performed at the Exxon Research and Engineering Co. Laboratory using an 18 kW rotating anode X-ray generator (Rigaku RU-300) with Cu K_α radiation, and a computer controlled Huber four-circle diffractometer. Different regions of a given sample were probed to determine the variation of the LLS with position. The area illuminated varied from 1×2 mm to $1{\cdot}5 \times 3$ mm. Layer orientation data are presented as plots of scattering intensity as $I(\beta)$ vs. β where β determines the sample orientation about an axis normal to the scattering plane, with a peak at $\beta = 0$ produced by layers normal to the plates. The LLS in the following cells were studied, the symbols referring to the indicated figures:

Figure 1 (*a*): A–SiO: ZLI-3654 (□, ○), SCE-3 (■, ●), and CS-1014 (◆).

Figure 1 (*b*): ZLI-3654; (□) brushed nylon surfaces (*planar* alignment), (△) P–SiO, (○) hybrid cell, one surface nylon the other oblique SiO.

Figure 1 (*c*): CS-1014; (○) *planar* alignment, (■) P–SiO.

2.2. *Observations: A–SiO cells*

In cells with *antiparallel* alignment of the SiO evaporation directions (A–SiO cells), only one scattering peak is present in the SA and SC phases, as shown in the typical data in figure 2 (*a*), in this case for ZLI-3654. This scattering is first detected as a single broad peak (full width at half height, FWHH = 17°) in $I(\beta)$ when the sample is cooled into the SA phase from the nematic. The corresponding layer tilt is large ($> 15°$) in comparison to cells with *planar* alignment. This uniform tilt of the layers increases monotonically with decreasing temperature, with the $I(\beta)$ peak narrowing

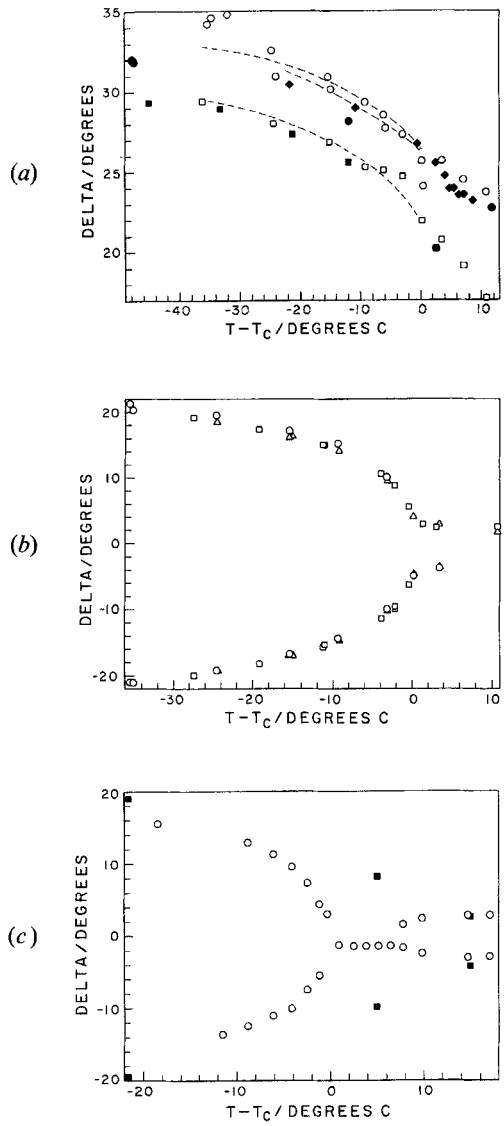

Figure 1. Layer tilt angle δ plotted as a function of $T - T_C$. (*a*) A–SiO cells, ZLI-3654 (□, ○), SCE-3 (■, ●), and CS-1014 (◆). The dashed curves are calculated for the three materials, using equation (1), assuming that the layer tilt $\delta(T)$ in the SC phase is governed by the initial tilt δ_0 at the SA–SC phase transition and the SC layer thickness $d_C(T)/d_A$. (*b*) ZLI-3654; (□) brushed nylon surfaces (planar alignment), (△) P–SiO, (○) hybrid cell, one surface nylon the other oblique SiO. (*c*) CS-1014; (○) *planar* alignment, (■) P–SiO. The data of (*b*), (*c*) and (*d*) enable $d_C(T)/d_A$ to be determined.

in the SC phase to a FWHH = 3° when the tilt has increased to 30° at 36°C below the SA–SC transition temperature, cf. figure 2 (*a*).

A single sharp peak in $I(\beta)$ indicates a uniform tilt of planar layers, which is what is found at the lower temperatures, well down into the SC phase. Figure 1 (*a*) shows the temperature dependence of this layer tilt for several different commercial FLC mixtures, showing that in general $\delta(T)$ increases with decreasing temperature.

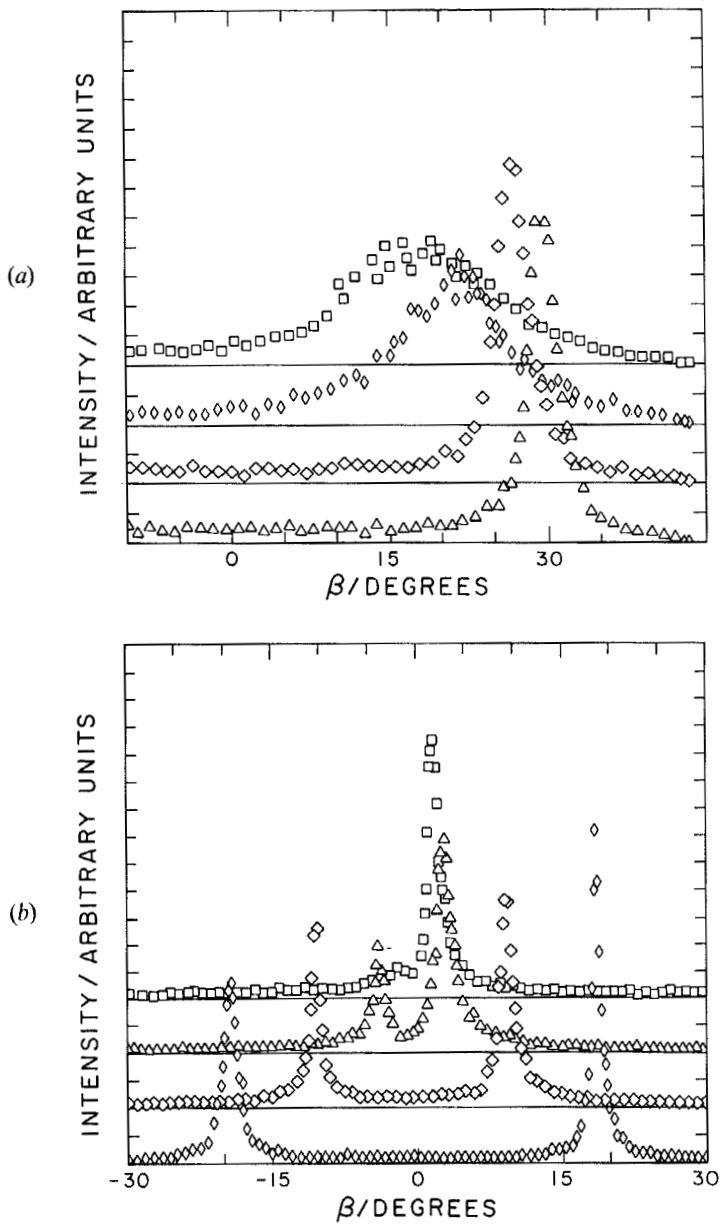

Figure 2. Typical data plotted as intensity $I(\beta)$ vs. β, the sample orientation. (*a*) ZLI-3654, A–SiO (corresponding to (□) in figure 1 (*a*): (□) $T = T_C + 10{\cdot}9°C$, (◇) $T = T_C + 0{\cdot}3°C$, (◇) $T = T_C - 15{\cdot}1°C$, (△) $T = T_C - 36{\cdot}1°C$. (*b*) ZLI-3654, P–SiO (corresponding to (△) in figure 1 (*b*): (□) $T = T_C + 10{\cdot}8°C$, (△) $T = T_C + 3{\cdot}6°C$, (◇) $T = T_C - 3°C$, (◇) $T = T_C - 24{\cdot}4°C$.

2.3. *Observations: P–SiO cells*

In cells with parallel alignment of the SiO surface treatment (P–SiO cells), two scattering peaks, disposed symmetrically in position about $\beta = 0$, but of different intensity, are observed in $I(\beta)$ in the SA and SC phases as shown for ZLI-3654 in

figure 2 (*b*). These peaks are narrow, with a FWHH of 2° in the SA phase at T_C + 10·8°C and decreasing to 1° in the SC phase at T_C − 24.4°C. The corresponding layer tilts increase monotonically as the sample is cooled through the SC phase. The appearance of symmetric peaks in $I(\beta)$ is reminiscent of the case of *planar* alignment and figure 1 (*b*) and (*c*) shows a comparison of P–SiO and *planar* layer tilts $\delta(T)$ for ZLI-3654 and CS-1014 respectively.

3. Discussion

3.1. *A–SiO cells: layer structure*

In the A–SiO cells the surface preferred director orientation on each plate is parallel to that on the other plate. This leads to a uniform director field in the nematic phase, pretilted by $\approx 20°$ from the surface plane, and upon cooling produces layers having a comparable average tilt δ in the SA phase; see figure 3 (*a*). The tilt angle δ increases with decreasing temperature in the SA phase for reasons which are presently unclear. The peaks are generally quite broad in the SA phase, possibly a result of focal conic layer curvature.

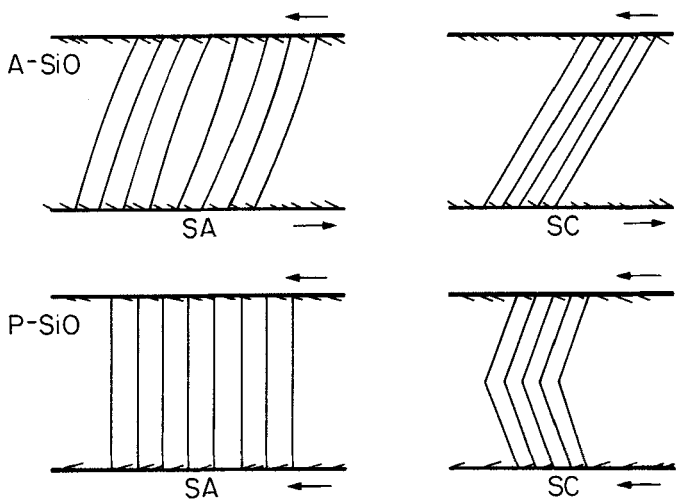

Figure 3. Sketches of the local layer structures found in (*a*) A–SiO cells and (*b*) P–SiO cells. At T_C the layers are dislocation free and have a tilt δ_0 equal to or less than the surface director tilt. Thermal contraction of the layers upon cooling in the SC phase results in the SC structures depicted.

The layer tilt $\delta(T)$ continues to increase with decreasing temperature in the SC phase (figure 3 (*a*)), with a variation that can be attributed to the strongly temperature dependent layer thickness $d_C(T)$. In general, upon cooling through the SA phase, the layers achieve some non-zero history dependent tilt δ_0 at T_C. Assuming that the layer pitch (number of layers/unit length along z) established at T_C is to be maintained in the SC phase, then, as the sample is further cooled, the layers shrink and, neglecting dislocations, must increase their angle of tilt $\delta(T)$ according to the following equation:

$$\cos(\delta) = \frac{d_C(T)}{d_A}\cos(\delta_0), \tag{1}$$

or, for small δ, δ_0

$$\delta \cong \sqrt{[\delta_p^2(T) + \delta_0^2]},$$

where

$$\delta_p(T) = \cos^{-1}\left(\frac{d_C(T)}{d_A}\right)$$

is the layer tilt found in planar cells, i.e. for $\delta_0 = 0$.

Figure 1 (*a*) presents data of layer tilt angle δ vs $T - T_C$ for three materials along with curves calculated from equation (1), using $d_C(T)$ and d_A data from planar cells. *The agreement shows that layer shrinkage controls layer tilt in the SC phase. This is as in planar cells but is not accompanied by chevron formation as in planar cells.* Chevrons form in *planar* aligned cells as a consequence of three conditions: (1) anchoring of the layers, i.e. no displacement at the bounding plates; (2) absence of layer dislocations; (3) shrinkage of the layers with decreasing temperature in the SC phase. The absence of chevrons indicates the breakdown of at least one of these conditions. A tentative explanation of this difference is realized if we consider the geometry of chevron formation in a cell with tilted surface orientations shown in figure 4. We assume that at T_C the layers are dislocation free and have a tilt δ_0 equal to or less than the surface director tilt Ω. Thermal contraction upon cooling in the SC phase causes δ to increase, which with the above conditions in force requires chevron formation via layer reorientation through the angle $-2\delta_0$ at one of the plates. In the SC phase near the SA–SC transition, the equilibrium bulk SC director tilt angle $\Theta(T)$ is small and this layer reorientation cannot take place while maintaining a director orientation at this surface which simultaneously satisfies the bulk SC tilt cone (constant $\hat{n} \cdot \hat{z}' = \cos\Theta(T)$) and surface preference constraints. The constraint can be satisfied for sufficiently large $\Theta(T)$, i.e. when $\Theta(T) > \delta_0 + \delta(T)$, where we have taken $\Omega = \delta_0$. Using the relation typically found [9] between $\Theta(T)$ and the SC layer thickness

$$\Theta(T) = r\cos^{-1}\left(\frac{d_C(T)}{d_A}\right)$$

with $r \sim 1{\cdot}2$, this inequality reduces to

$$\Theta(T) > \cos^{-1}\left(\cos\frac{\Theta(T)}{r}\cos\delta_0\right) + \delta_0.$$

Using small angle approximations we find:

$$\Theta > \frac{2r^2\delta_0}{r^2 - 1} \sim 7\delta_0. \tag{2}$$

Because Θ increases more rapidly than δ, the condition for chevron formation can in principle be met for sufficiently large $\Theta(T)$, i.e. sufficiently far down in the SC phase according to equation (2). However, for most SA–SC materials we have $\Theta(T) \lesssim 30°$, so that for $\Omega = \delta_0$ greater than a few (~ 5) degrees, the condition cannot be met in practice and chevrons do not appear, the excess surface energy suppressing their formation. The result is a loss of one of the three above conditions. Since the X-ray data indicates that the layers have the expected temperature dependence of $d_C(T)$, i.e. that (3) still holds and that $\Theta(T)$ vs $d_C(T)$ obeys equation (1), indicating that (2) still holds, it must be (1) that is lost.

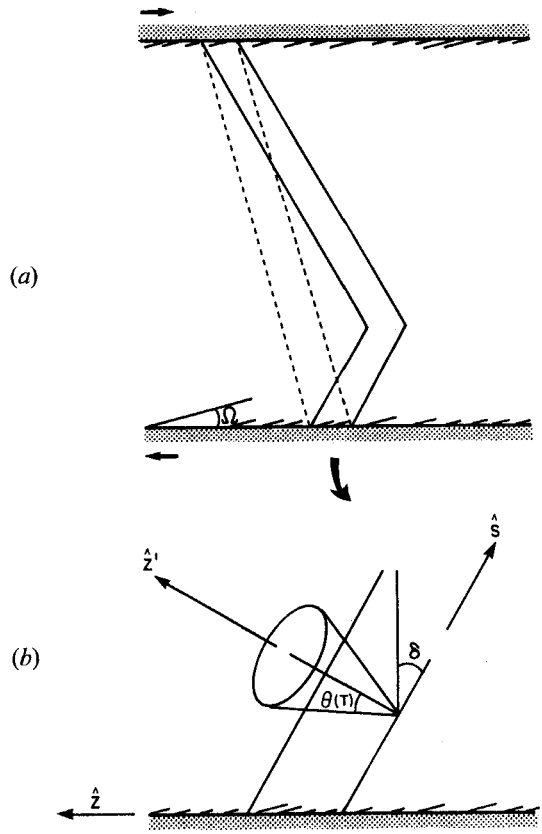

Figure 4. (*a*) Chevron formulation in cells with antiparallel SiO or rubbed plates. The director in the nematic and SA phases is uniform and tilted out of the planes of the bounding plates. Upon cooling and entering the SC phase the layers are initially tilted through an angle δ_0. To form a chevron the geometry requires a layer reorientation at one or the other of the surfaces through the angle $2\delta_0$; (*b*) If δ_0 is too large (see equation (2)) at the surface the director cannot simultaneously lie on the bulk SC tilt cone and have the preferred orientation $\Omega - \delta_0$ relative to the surface.

Returning to figure 2 (*a*), the narrowing of the $I(\beta)$ peak with increasing δ is quite striking. At T_C a distribution of δ_0s over the range 15·6°–26·4° is observed, narrowing to 3°, 36·1°C below T_C. One possible origin of this effect is that, as the layers shrink in the SC phase, the tilt angles $\delta(T)$ obeying equation (1) for various δ_0s collapse into a narrower range. However figure 5, shows this not to be the case, with the net increase in δ being nearly independent of the starting δ_0. This would appear to rule out a mosaic of regions of differently oriented planar layers as the origin of the broadening of $I(\beta)$ at higher temperatures, since from figure 5, the peak width would hardly change if this was the case. Rather, this evidence points to locally curved layers in the SA phase and a relaxation to planar layers with decreasing temperature.

3.2. *A–SiO cells: optical observations and director field structure*

Observations in transmission polarized microscopy show that A–SiO cells lack zig-zag walls, consistent with the A–SiO cell uniform tilted layer structure and the

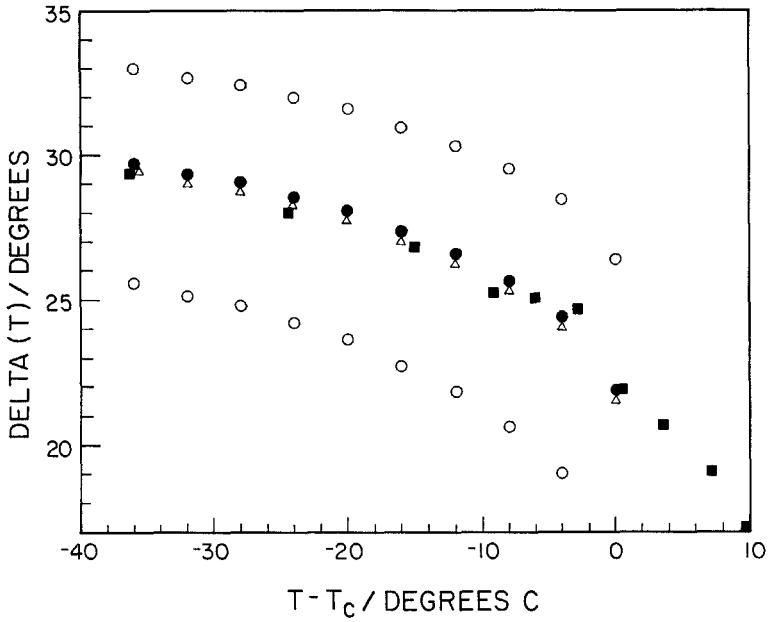

Figure 5. Plot of δ vs. $T - T_C$. ■ data for A–SiO cell filled with ZLI-3654 (the same as in figure 1 (*a*). All other curves are data calculated from equation (1) with differing values of δ_0. ● points are for δ_0s calculated from the ratio of the cosine at $\delta_p(T)$, the layer tilt for *planar* alignment, to the cosine of $\delta_t(T)$, the layer tilt for an A–SiO cell. The △ and both sets of ○ data points are for δ_0s taken as the peak, lower FWHM, upper FWHM, respectively from figure 2 (*a*), (◇) curve.

requirement of chevron layers for zig-zags. Application of electric fields to A–SiO cells shows a splayed **n-P** structure stabilized by polar surface interactions [3, 16] in the limit of small electric field, with surface domain mediated orientation transitions at one (the other) of the FLC-solid interfaces to uniform up (down) states at large + (−) electric fields.

The structure of the director-polarization **n-P** field in A–SiO cells with tilted planar layers is determined by conditions at the FLC-solid interfaces, namely by the geometry of the tilt cone and preferred surface orientation constraints. This geometry is shown in figure 6 (*a*).

3.3. *P–SiO cells: layer structure*

Figure 1 shows the layer tilt scenarios found in the P–SiO cells. In general the P–SiO treatment produces the chevron structure in the SC phase. In the SA phase the layer structure varies from sample to sample, depending on sample history, with layer tilts ranging from zero to 15° in different samples. Thus, in contrast to the A–SiO surfaces, with P–SiO the SA layer tilts are not directly related to the surface tilt imposed by the boundary condition, presumably because, in the SA phase, both boundary conditions cannot be satisfied simultaneously with plane layers, as is possible with A–SiO. The layer structure adopted in P–SiO depends on the layer growth scenario at the N–SA transition. Figure 1 (*b*) shows typical results when the layer tilt is small in the SA phase. The $\delta(T)$ curves for P–SiO, *planar* alignment (rubbed nylon), and a hybrid cell are essentially the same, indicating that the layer

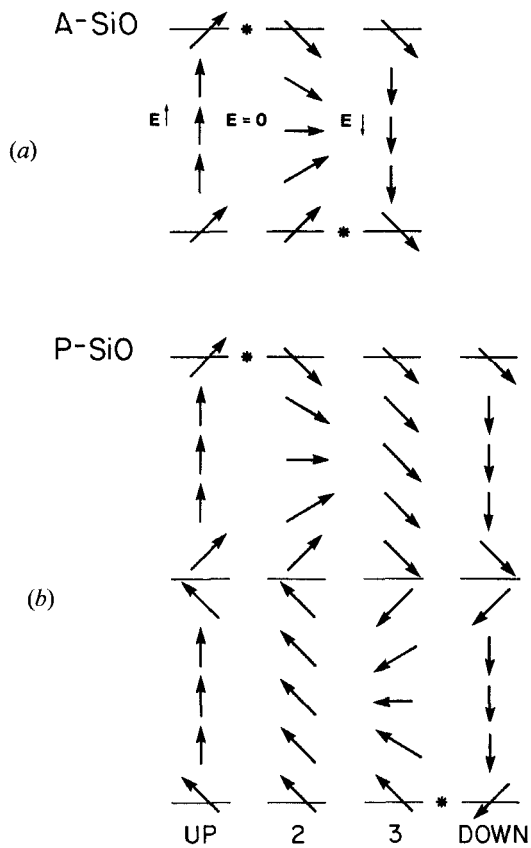

Figure 6. (*a*) A–SiO cells generally have a monostable equilibrium splayed state at $E = 0$ with **P** directed into or out of the surface (dependent on the material). Sufficiently strong applied fields produce surface domains (*) which mediate switching between nearly uniform UP and DOWN states. Possible variations of this scenario are discussed in [2]. (*b*) P–SiO cells exhibit the 4-state switching behaviour characteristic of the chevron structure.

thickness controls $\delta(T)$ in all three cases. Figure 1 (*c*) shows a case where the chevron structure is established with a large layer tilt. In this case the boundary conditions are simultaneously partially satisfied by chevron formation and the tilt angle increase with decreasing T in the SC phase depends on the layer pitch established at the SA–SC transition, i.e. according to equation (1).

3.4. *P–SiO cells: optical observations and director field structure*

Optically P–SiO cells are zig-zag defect free and exhibit domain mediated transitions at the two FLC-solid interfaces and at a third internal interface, as found in *planar* aligned cells having chevron layers and an internal chevron interface [5, 6, 10].

This observation, along with the X-ray results of symmetrically tilted layers indicates that the layers in the P–SiO cells have the chevron structure. Since zig-zags mediate the change in chevron direction, the absence of zig-zag defects indicates the presence of a single chevron direction in P–SiO cells, as might be expected since the surface pretilt condition breaks the energy degeneracy of the <<< and >>> chevron states.

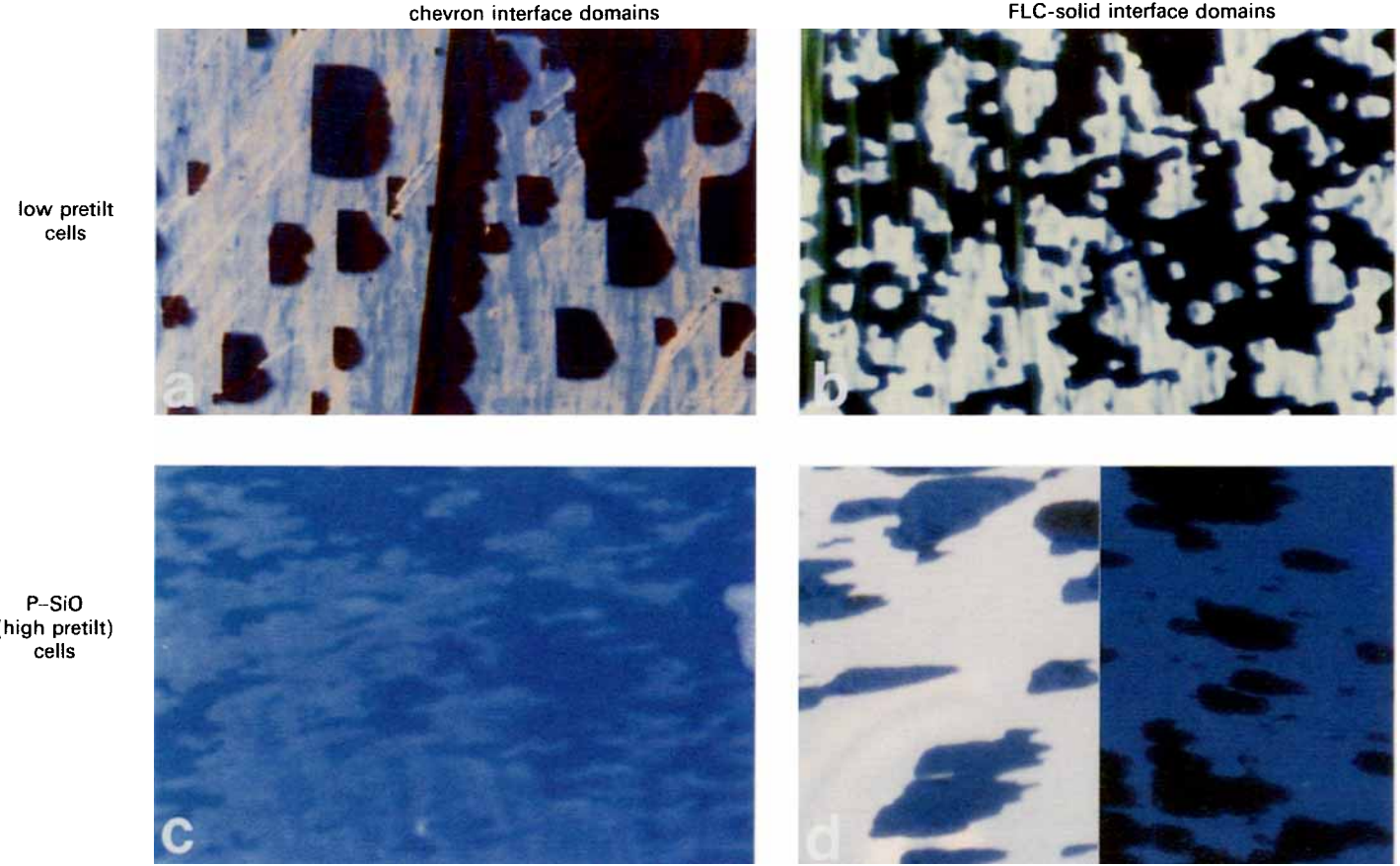

Figure 7. Comparison of domain walls at the chevron and the FLC-solid interfaces in low pretilt case the high contrast domains are at the chevron interface (switching from state 2 → 3 in figure 6 (*b*)) and have a characteristic boat shape (*a*), and the FLC-solid surface transition domains (2 → UP in figure 6 (*b*)) are irregularly shaped (*b*). In the P–SiO cells the chevron (2 → 3) domains have very little contrast and have irregular shapes (*c*), while the FLC-solid (2 → UP) domains have a characteristic triangular (shoe) shape (*d*). The photomicrographs of (*d*) show both the 2 → UP (blue–white) and the 3 → DOWN (blue–black) domains. The SC layers run horizontal in all photos.

The switching characteristics in the **n-P** fields in the P–SiO cells are somewhat different from those of chevron cells having *planar* (low pretilt) surfaces, such as clean indium tin oxide or rubbed polymer. In the latter the chevron interface switches at low field with the characteristic boat shaped domains [17] shown in figure 7 (*a*) and this switching between states 2 and 3 [10] in figure 6 (*b*) produces significant contrast. The surface transitions occur via surface domains at higher fields (state 2 → UP and state 3 → DOWN) and produce much less contrast, since the surface disclinations which appear via the domains are quite thin. The surface domains are generally irregular in shape as shown in figure 7 (*b*). The chevron domains have much higher mobility than the surface domains.

In the P–SiO cells as in the low pretilt chevron cells three switching transitions are found, with the 2 ↔ 3 transition on the chevron interface (the one occurring at low voltage) producing rather little contrast and exhibiting irregularly shaped high mobility domains; see figure 7 (*c*). On the other hand the (2 → UP and 3 → DOWN) surface transitions produce significant contrast in the P–SiO cells. Additionally, the surface domain has a characteristic triangular shape as shown in figure 7 (*d*). Similar domain behaviour has been reported for P–SiO cells by Yamada *et al.* [18].

The origin of these differences is not entirely clear at the present time. Since the layer tilt angles are the same for the two preparations the **n-P** boundary conditions at the chevron interface should be the same in the two cases. On the other hand the boundary conditions at the FLC-solid interfaces are likely to be quite different. Applying the arguments of Handschy and Clark [3] it would appear that qualitatively the nonpolar anchoring energy is weaker in the case of P–SiO than for the other low pretilt surface treatments. Thus in P–SiO the surface transition occurs at lower field with a correspondingly thicker surface disclination layer [3]. Additionally the higher surface domain contrast indicates surface switching through a larger angle in the P–SiO case. With typical low pretilt alignment the polarization pretilt ϕ_p at the surface is $\phi_p \sim 45°$ (ϕ_p is the angle between **p** and $\hat{s}$ in figure 4), using $\theta \sim 30°$, $\delta \sim 1{\cdot}25\Theta$, and $\Omega = 0$ in

$$\sin \phi_p - \frac{\tan(\delta - \Omega)}{\tan \Theta}, \tag{3}$$

where Ω is the angle between the director and surface plane. The surface switching in this case produces a change ϕ of about 90°. In the P–SiO case if the strongest surface attractor is conical with an angle of $\Omega \sim 25°$ between the director and surface as recently proposed by Durand [19], then $\delta - \Omega$ is small, ϕ_p will be close to 0°, and the change is ϕ at the surface upon switching close to 180°. This should produce a larger optical effect upon switching as found.

The observations of figure 7 show that the domain walls having significant contrast (i.e. a substantial change in the **n-P** field) have a particular domain wall shape —that is both interface and bulk factors determine the structure of the boat shaped domain on the chevron of figure 7 (*a*) and the shoe shaped surface domain of figure 7 (*d*).

This work was supported by NSF grant No. DMR 8901657, NSF grant CDR 8622236 through the National Science Foundation Engineering Research Center for Optoelectric Computing Systems, and ARO contrast DAAL 03-86-0053.

References

[1] Clark, N. A., and Lagerwall, S. T., 1980, *Appl. Phys. Lett.*, **36**, 899.
[2] Clark, N. A., and Lagerwall, S. T., 1984, *Ferroelectrics*, **59**, 25.
[3] Handschy, M. A., and Clark, N. A., 1984, *Ferroelectrics*, **59**, 69.
[4] Rieker, T. P., Clark, N. A., Smith, G. S., Parmer, D. S., Sirota, E. B., and Safinya, C. R., 1987, *Phys. Rev. Lett.*, **59**, 2658.
[5] Clark, N. A., and Rieker, T. P., 1988, *Phys. Rev.* A, **37**, 1053.
[6] Rieker, T. P., 1988, Ph.D. thesis, University of Colorado, Boulder (to be published).
[7] Urbach, W., Boix, M., and Guyon, E., 1974, *Appl. Phys. Lett.*, **25**, 479.
[8] Uemura, T., Ohba, N., Wakita, N., Ohnishi, H., and Ota, I., 1986, *Japan Display '86*, p. 464.
[9] Hauck, G., 1987, *Crystal Res. Technol.*, **22**, 817.
[10] Clark, N. A., Rieker, T. P., and Maclennan, J. E., 1988, *Ferroelectrics*, **85**, 79.
[11] Ouchi, Y., Lee, J., Takezoe, H., Fukuda, A., Kondo, K., Kitamura, T., and Mukoh, A., 1988, *Jap. J. appl. Phys.*, **27**, 5.
[12] Ouchi, Y., Lee, J., Takezoe, H., Fukuda, A., Kondo, K., Kitamura, T., and Mukoh, A., 1988, *Jap. J. appl. Phys.*, **27**, 11.
[13] Chisso 1014 is a proprietary mixture, available from Chisso with the phase I $\overset{81°}{\longleftrightarrow}$ Ch $\overset{68°}{\longleftrightarrow}$ SA $\overset{54°}{\longleftrightarrow}$ SC*.
[14] ZLI-3654 is a proprietary mixture, available from E. Merck, with the phase sequence I $\overset{86°}{\longleftrightarrow}$ Ch $\overset{76°}{\longleftrightarrow}$ SA $\overset{62°}{\longleftrightarrow}$ SC*.
[15] SCE-3 is a proprietary mixture, available from BDH, with the phase sequence: I $\overset{136°}{\longleftrightarrow}$ Ch $\overset{105°}{\longleftrightarrow}$ SA $\overset{74°}{\longleftrightarrow}$ SC*.
[16] Handschy, M. A., Clark, N. A., and Lagerwall, S. T., 1983, *Phys. Rev. Lett.*, **51**, 471.
[17] Ouchi, Y., Takezoe, H., and Fukuda, A., 1985, *Jap. J. appl. Phys.*, **26**, 1. Ishikawa, K., 1985, *Jap. J. appl. Phys.*, **24**, L230.
[18] Yamada, Y., Tsuge, T., Yamamoto, N., Yamawachi, M., Orihara, H., and Ishibashi, Y., 1988, *Ferroelectrics*, **85**, 123.
[19] Durand, G., 1988, *Second International Topical Meeting on Optics of Liquid Crystals*, Torino.